Provisional chapter

Neurodegenerative Diseases Associated with Mutations in *SLC25A46*

Zhuo Li, Jesse Slone, Lingqian Wu and Taosheng Huang

Additional information is available at the end of the chapter

Abstract

Neurodegenerative diseases present substantial clinical challenges. Their processes have been linked with various genetic causes, including mutations of genes encoding proteins associated with mitochondrial dynamics. Biallelic mutations in *SLC25A46* have been identified as novel causes of a wide spectrum of neurological diseases with recessive inheritance, including optic atrophy, Charcot-Marie-Tooth neuropathy (CMT) type 2A neuropathy, Leigh syndrome, progressive myoclonic ataxia, and lethal congenital pontocerebellar hypoplasia. SLC25A46 (solute carrier family 25 member 46) is a membrane transit protein that is expressed in the mitochondrial outer membrane where it plays a major role in mitochondrial dynamics and cristae maintenance. This chapter presents recent findings on: (1) the clinical heterogeneity of SLC25A46-related neuropathies; (2) the *SLC25A46* mutation spectrum and associated genotype-phenotype correlation; and (3) pathophysiological functions of SLC25A46 as characterized in cells and mouse models. A better understanding of the etiology of *SLC25146*-linked diseases will elucidate therapeutic perspectives.

Keywords: neurodegeneration, SLC25A46, mitochondrial dynamics, optic atrophy, CMT-2 neuropathy, pontocerebellar hypoplasia

1. Introduction

Mitochondria have long been recognized as critical organelles for cellular energy generation. They produce ~90% of neuronal adenosine triphosphate (ATP), which is continuously required for maintaining the complex morphology and specialized functions of neurons, including electrical excitability and synaptic transmission [1], and are regenerated continuously in postmitotic

neurons through biogenesis. In addition to undergoing the dynamic processes of mitochondrial fission and fusion, mitochondria are transported bidirectionally within neurites, in which they are distributed purposefully, facilitating energy transmission over long distances to meet local demands and, when necessary, undergo controlled degradation by mitophagy [2, 3]. Thus, mitochondrial dynamics play critical roles in neuronal homeostasis and survival.

Recent evidence suggests that abnormal mitochondrial dynamics may contribute to both familial and sporadic neurodegenerative diseases [4]. Most proteins related to mitochondrial dynamics are encoded by genes in the nucleus. Mutations in such nuclear-encoded genes can cause monogenic disorders in which mitochondrial dysfunction is unequivocally central to the pathogenesis of the disease. For example, mutations in *MFN1/2* and *OPA1* cause Charcot-Marie-Tooth neuropathy (CMT) type 2A [5–7] and autosomal dominant optic atrophy (ADOA) [8–10], respectively. A dominant negative allele of *DRP1* was identified in a neonate with a lethal mitochondrial and peroxisomal fission defect associated with abnormal brain development, optic atrophy, and various other congenital anomalies [11]. Defects in proteins involved in axonal transport have also been identified in patients with CMT and related neuropathies [12–14]. In addition, there is increasing evidence linking mitochondrial dysfunction to neuronal loss in age-related neurodegenerative disorders, including Alzheimer's disease and Parkinson's disease [15, 16].

Recent studies have implicated the 46th isoform of subfamily A of the solute carrier (SLC) family 25, termed SLC25A46, in mitochondrial dysfunction pathology. SLC25A46 is a mitochondrial outer membrane protein that was shown recently to be involved in mitochondrial dynamics, either playing a role in mitochondrial fission or serving as a regulator of mitofusin (MFN)1/2 oligomerization [17, 18]. Disorders caused by recessive *SLC25A46* mutations were defined recently as a new syndrome (introduced and elaborated in Section 3.1) that has a broad clinical spectrum of neurological phenotypes, including peripheral neuropathy, early-onset optic atrophy, cerebellar degeneration, and congenital pontocerebellar hypoplasia (PCH), with variable ages of onset and severities [17, 19–26]. In this chapter, we will focus on the phenotypic and genetic characteristics of *SLC25A46*-related neurological diseases and our current understanding of the pathophysiological mechanisms linking dysfunctional SLC25A46 to neurodegeneration.

2. SLC25 family and the discovery of *SLC25A46*

SLC25A46 belongs to the solute carrier family 25 (SLC25), a superfamily that contains 53 nuclear-encoded mitochondrial carrier proteins in humans [27]. SLC25 members are characterized by the presence of three tandem repeats of about 100 amino acids, each containing two transmembrane alpha helices linked by a large loop [28]. The mature carrier protein thus consists of six transmembrane helices that form an aqueous pore and have a highly conserved consensus sequence, P-X-[D/E]-X-X-[R/K], at the C-terminal ends of the three odd-numbered transmembrane alpha helices, whose charged residues form salt bridges that close the pore on the matrix side [29]. SLC25 proteins may shuttle a variety of solutes across the mitochondrial

membrane to participate in various metabolic pathways [30]. Although common mechanisms of substrate translocation have been proposed, SLC25 members vary greatly in their size, the nature of substrates they transport, the modes of transport employed, and the driving forces they employ [30–32].

A number of genetic conditions associated with SLC25 mitochondrial transporters have been characterized biochemically and genetically [33]. SLC25 members mediate a variety of cellular functions, and mutations in SLC25 genes have been linked to various defects, such as carnitine/acylcarnitine carrier deficiency (OMIM 212138), HHH syndrome (OMIM 238970), aspartate/glutamate isoform 1 and 2 deficiencies (OMIM 612949, 603471, 605814), congenital Amish

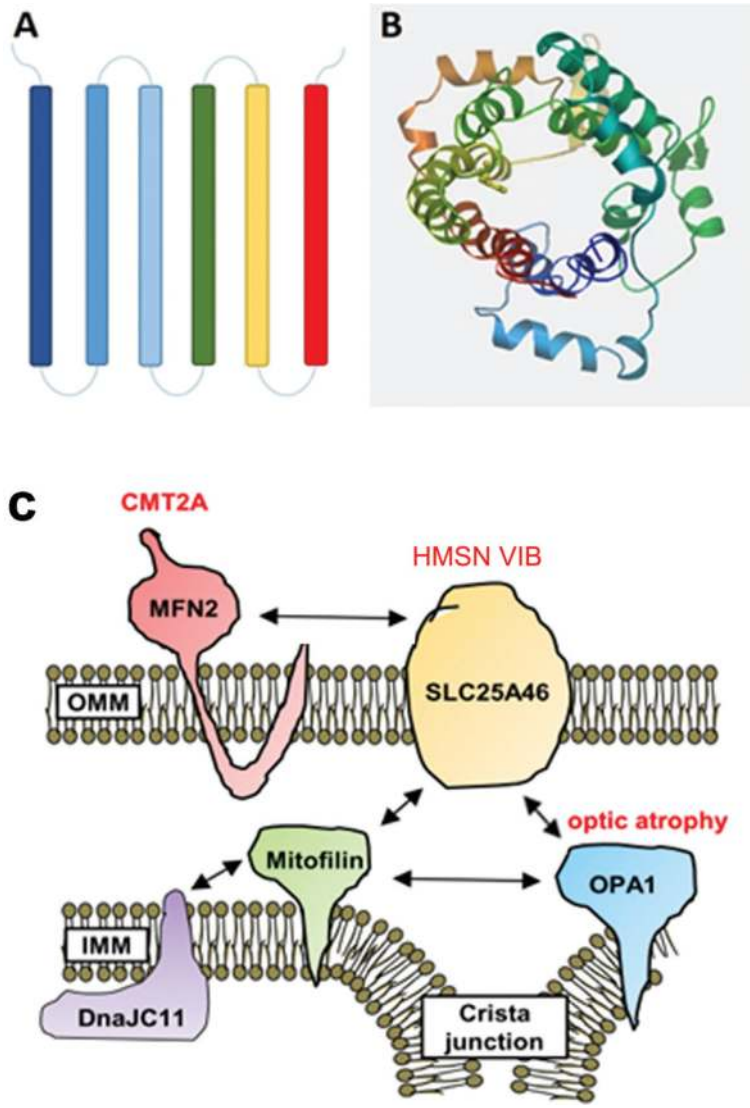

Figure 1. Schematic diagram of SLC25A46 structure and its interactions. (A) SLC25A46 consists of six conserved transmembrane alpha helices. (B) 3D structure of SLC25A46. (C) Potential interactions of SLC25A46 with dynamic proteins.

microcephaly (OMIM 607196), neuropathy with bilateral striatal necrosis (OMIM 613710), congenital sideroblastic anemia (OMIM 205950), neonatal epileptic encephalopathy (OMIM 609304), and citrate carrier deficiency (OMIM 190315) [33]. These disorders are characterized by specific metabolic dysfunctions related to the role of the particular carrier that has been affected. Most disease-related SLC25 members have been characterized in terms of substrate identification and associated metabolic pathways, with the exception of two orphan SLC25 members, namely SLC25A38 and SLC25A46 [33].

SLC25A46 was first mapped to chromosome 5 by genomic sequence analysis in 2006 [27]. Its location was further refined to chromosome 5q22.1 based on sequence alignment with NCBI's standard reference human assembly sequence, that is, the Genome Reference Consortium Human genome build 38. The largest transcript isoform of *SLC25A46* contains eight exons, which encode a 418-amino acid protein. Quantitative real-time polymerase chain reaction (PCR) experiments in rodents have demonstrated variable expression of *SLC25A46* in all tissues examined, with the highest levels occurring in the hindbrain, spinal cord, and coronal brain sections containing the corpus callosum, fornix, optic chiasm, thalamus, hypothalamus, midbrain, pons, and cerebellum, with particularly high levels in mouse embryo cerebellum [27].

Given the typical SLC25 molecular structure, the primary sequence of the SLC25A46 protein has been predicted to form six conserved transmembrane alpha helices, TM1–TM6, spanning a region between amino acids 100–418 (**Figure 1**) [22]. However, the otherwise highly conserved P-X-(D/E)-X-X-(R/K) consensus sequence characteristic of SLC25 proteins is altered in SLC25A46. Moreover, the N-terminus of SLC25A46 is about five times longer than that of other members of the family (∼100 vs. <20 amino acids). These unusual characteristics suggest that SLC25A46 is unlikely to have a conventional metabolite carrier function. Recently, studies have proposed that unlike most SLC25 members that are located in the inner mitochondrial membrane, SLC25A46 may be anchored to the outer mitochondrial membrane where it may act as a regulator of mitochondrial dynamics rather than as a substrate transporter.

3. Clinical phenotypes of *SLC25A46*-related diseases

3.1. Hereditary motor and sensory neuropathy type VIB (HMSN6B)

In 2015, recessive mutations in *SLC25A46* in eight patients from four unrelated families of various ethnic origins were first reported. The proband phenotypes encompassed ADOA-like optic atrophy, CMT-like axonal peripheral neuropathy, and cerebellar atrophy with a variable age of onset and disease course (**Table 1**) [17]. This new neurodegenerative syndrome is now defined as HMSN6B in OMIM (OMIM: 616505). ADOA and CMT type 2 are hereditary neurodegenerative disorders commonly caused by mutations in the mitochondrial fusion genes *OPA1* and *MFN2*, respectively. However, both diseases lack a genetic diagnosis in up to 60% of patients due to genetic heterogeneity [34, 35].

SLC25A46 provides a new locus in genetic testing for patients with ADOA and CMT-like phenotypes. Indeed, four independent clinical reports published in 2016 and 2017 identified

ID	SLC25A46 mutations	SLC25A46 proteins	Age of onset	Age of death	Optic atrophy	Peripheral neuropathy	Cerebellar or brainstem atrophy	Hypotonia or myopathy	Ataxia	Lactate	Other features	Mitochondrial dynamics
UK family Abrams et al. [17]	c.165_166insC; c.746G>A	p.His56fs*94; p.Gly249Asp	5 y/8 y	Alive (40 y/43 y)	+	+	–	–	–	Normal	Normal CSF examination, oxidative enzyme activity, no ragged red fibers.	n.k.
PL family Abrams et al. [17]	c.1005A>T	p.Glu335Asp	1 y/2 y	Alive (13 mo/11.5 y)	+	+	+	+	+	↑	Developmental delay, 3-MG ↑ in urine.	Increased mitochondria.
IT family Abrams et al. [17]	c.1018C>T	p.Arg340Cys	2 y	Alive (51 y)	+	+	+	+	+	↑	CK ↑(225, NR<170 U/L), lactic acid at upper end of normal range.	Hyperfilamentous.
US family Abrams et al. [17]	c.882_885dupTTAC; c.998C>T	p. Asn296fs*297; p.Pro333Leu	Prenatal	105 d	+	+	+	+	n.k.	n.k.	Facial and hand dysmorphism, meconium aspiration.	n.k.
Moroccan family Nguyen et al. [21]	c.283+3G>T	p.?	Prenatal	7 d	+	n.k.	+	+	n.k.	↑	Club foot posture, lactate-to-pyruvate ratio ↑ and all individual complexes ↓ in fibroblasts.	Mitochondrial fragmentation.
Pakistani origin family Charlesworth et al. [19]	c.413T>G	p.Leu138Arg	n.k.	Alive (15 y/20 y)	+	+	+	+	+	n.k.	Comprised exotropia, difficulty initiating saccades, spasticity, scoliosis. Old brother with mild phenotypes.	n.k.
Saudi family Sulaiman et al. [26]	c.775C>T	p.Arg259Cys	28 y	Alive	+	–	–	+	n.k.	Normal	No ragged red fiber or cytochrome c deficiency, intact sensation and coordination, unremarkable acylcarnitine profile, amino acids, CK and urine organic acids.	Occasional enlarged mitochondria.
Tunisian family Hammer et al. [23]	c.1018C>T	p.Arg340Cys	1 y/6 y	Alive (22 y/19 y)	+	+	±	n.k.	+	n.k.	Dysarthria, gait instability, Babinski sign, abolished Achilles reflexes, finger-nose dysmetria, severe sensorimotor demyelination.	n.k.

ID	SLC25A46 mutations	SLC25A46 proteins	Age of onset	Age of death	Optic atrophy	Peripheral neuropathy	Cerebellar or brainstem atrophy	Hypotonia or myopathy	Ataxia	Lactate	Other features	Mitochondrial dynamics
Algerian family 1 Hammer et al. [23]	c.1018C>T	p.Arg340Cys	2 y	Alive (31 y)	+	+	±	n.k.	+	n.k.	Subtle white matter changes in cerebellum, increased tendon reflexes, no Achilles reflex, positive Hoffmann sign, no Babinski sign.	n.k.
Algerian family 2 Hammer et al. [23]	c.479G>C	p.Trp160Ser	23 y	Alive (26 y)	−	n.k.	n.k.	n.k.	+	n.k.	Abolished vibration sense, at ankles, nystagmus and saccadic pursuit, scoliosis.	n.k.
Family 1 Wan et al. [22]	c.1022T>C	p.Leu341Pro	Prenatal	14 d/28 d	n.k.	n.k.	+	+	n.k.	Normal	PCH, severe global developmental delay, normal respiratory chain enzymes in muscle and liver.	Increase in mitochondrial length.
Family 2 Wan et al. [22]	g.chr5:110738771_ 11074670del	p.?	Prenatal	42 d	+	+	+	+	n.k.	↑	PCH, occasional myoclonic jerks; EEG: generalized slowing with abnormal theta rhythm, no epileptic discharges, sibling with same phenotype.	n.k.
Dutch family Dijk et al. [25]	c.691C>T g.chr5:110742638_ 110745029del	p.Arg231*; p.?	Prenatal	1 d	+	n.k.	+	+	n.k.	n.k.	PCH, all three children died within 1 day after birth, lack of spontaneous respiration, profound muscle weakness. Convulsion, spinal motor neuron degeneration.	n.k.
German family Braunisch et al. [24]	c.736A>T	p. Arg 246 *	Prenatal	1 d/23 d	n.k.	n.k.	+	+	n.k.	↑	PCH, seizures, EEG: low amplitudes with sharp waves, epileptiform discharges without clinical equivalents, thrombocytes ↑, lung hypoplasia,	n.k.

ID	SLC25A46 mutations	SLC25A46 proteins	Age of onset	Age of death	Optic atrophy	Peripheral neuropathy	Cerebellar or brainstem atrophy	Hypotonia or myopathy	Ataxia	Lactate	Other features	Mitochondrial dynamics
											bradycardia at birth, green amniotic fluid.	
Italian family Braunisch et al. [24]	c.42C>G; c.462+1G>A	p.Tyr14 *; P. ?	Prenatal	1 d/18 d	n.k.	n.k.	+	+	n.k.	n.k.	PCH, floppy infant, little respiratory effort and voluntary movements; EMG: neurogenic lesion; loss of spinal motor neurons, normal CK levels, serum transferrin IEF, two siblings were hypotonic and died immediately after birth.	n.k.
French Canadian family Janer et al. [20]	c.425C>T	p.Thr142Ile; (instable protein)	Birth	15 mo	+	n.k.	+	+	n.k.	↑	Leigh syndrome, psychomotor delay, growth retardation, mild spastic diplegia; motor delay; fever, convulsion, gasping respirations, bilateral intranuclear ophthalmoplegia, hyperreflexia, mild spasticity.	Mitochondrial hyperfusion in fibroblast.

Note: y, year; mo, month; d, day; n.k., not known; ↑, increase.

Table 1. Clinical phenotypes associated with SLC25A46 mutations.

homogenous *SLC25A46* mutations in an additional nine patients (age range, 7 days to 28 years) from five unrelated families who presented with neurological phenotypes similar to the core features of HMSN6B. Among these nine patients, eight had optic atrophy (the exception was a patient with an age of onset 23 years) and eight had cerebellar atrophy (the exception was a 28-year-old patient without remarkable cerebellar atrophy or axonal neuropathy) (**Table 1**) [19, 21, 23, 26]. Beyond the key clinical features of optic atrophy, peripheral neuropathy, and cerebellar atrophy, the presently documented population of 17 patients with HMSN6B (or an HMSN6B-like condition) exhibited other clinical symptoms sporadically, including ataxia, hypotonia, myoclonus, dysmetria, nystagmus, speech difficulties, abnormal brain imaging, and elevated lactic acid (**Table 1**). The clinical manifestations, medical examination findings, and differential diagnoses for these patients were strongly suggestive of a progressive mitochondrial disorder.

3.2. *SLC25A46*-related PCH and Leigh syndrome

A recent study reported the identification of *SLC25A46* loss-of-function mutations in four patients from two unrelated families with a diagnosis of severe congenital PCH, leading to very early mortality [22]. Then, two independent groups reported an additional seven patients from three unrelated families with severe PCH associated with truncating mutations of *SLC25A46* (**Table 1**) [24, 25].

PCH is a rare, heterogeneous group of prenatal onset neurodegenerative disorders, mainly (but not exclusively) affecting the cerebellum and pons. The current PCH classification scheme includes 10 distinct PCH subtypes defined by clinical features and genetic etiology. PCH1 is distinguished from the other PCH subtypes by its association with spinal muscular atrophy due to spinal motoneuron degeneration; it often leads to early death. All patients with obvious loss-of-function *SLC25A46* genotypes in the literature suffered severe lethal congenital PCH, presenting with the phenotypic hallmarks of cerebellar and brainstem degeneration as well as spinal muscular atrophy, respiratory failure, early death, occasional optic nerve atrophy, and axonal neuropathy. Based on these features, SLC25A46-associated PCH could be classified as PCH1, and perhaps a new PCH1 subtype, PCH1D, clinically distinguished from other PCH1 subtypes (mutations in *VRK1*, *EXOSC3*, and *EXOSC8* are associated with PCH1A, PCH1B, and PCH1C, respectively) [25]. However, the most severe clinical presentation associated with *SLC25A46* mutations is probably not restricted to PCH. A homozygous *SLC25A46* mutation that resulted in the complete absence of the protein was identified recently in a terminally ill child with progressive brain lesions consistent with those seen in Leigh syndrome (**Table 1**) [20].

Cerebellar and brainstem atrophy are shared phenotypic features of PCH, Leigh syndrome, and most variant *SLC25A46*-related HMSN6B cases. Meanwhile, optic nerve and peripheral nerve axonal pathology are seen consistently in HMSN6B. Features that are prominent in later-onset cases might be overlooked or not assessed in neonatally lethal cases. Thus, *SLC25A46*-related PCH or Leigh syndrome could be extreme forms of HMSN6B.

To sum up, *SLC25A46*-related neurological disease has high clinical heterogeneity. Patients with biallelic *SLC25A46* mutations show high phenotypic variability with respect to age of

onset, clinical features, and disease course. The severity of presentation even varies between siblings. The phenotype spectrum ranges from severe disease at birth with early death to manifestation in late childhood with survival beyond 50 years of age.

4. Mutation spectrum of *SLC25A46* and genotype-phenotype correlation

4.1. Mutation spectrum of *SLC25A46*

The *SLC25A46* gene, located on chromosome 5q22.1, spans approximately 27 kb and is composed of eight exons. The main protein isoform has 418 amino acids and is encoded by a 1257-nucleotide-long open reading frame. Since *SLC25A46* mutations associated with neurological disease were first reported in 2015, more than 28 patients with various mutations from 16 unrelated families have been diagnosed genetically, most by whole-exome sequencing, leading to the discovery of a total of 18 pathogenic mutations in the last 2 years (**Figure 2**). Of these, 50% are missense mutations; 16.7% are nonsense mutations; 11.1% are splice variants; and 22.2% are micro-deletions, insertions, or duplications. The mutation sizes range from a single nucleotide polymorphism to a 2.4-kb deletion. Although some mutations have been found in all exons except exons 2, 6, and 7, 50% of the mutations are located in exon 8, the largest exon, which accounts for half of the *SLC25A46* open reading frame (**Figure 2**). Although there is no suspected mutation hotspot site, the c.1081C>T variant was observed in 3 of 16 independent families (**Table 1**). The identification and genetic diagnosis of additional cases in the future may reveal a *SLC25A46* mutation pattern.

4.2. Genotype-phenotype correlation

A systemic genotype-phenotype analysis of all available cases indicates that phenotype severity correlates strongly with the magnitude of SLC25A46 protein level reduction caused by each

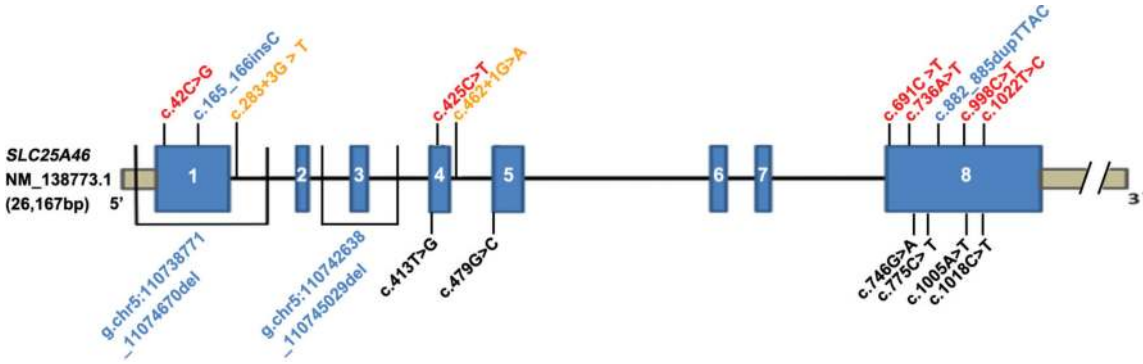

Figure 2. Schematic diagram of reported pathogenic SLC25A46 variants. Exons 1–8 are represented by blue blocks. Mutations are color coded as follows: red, nonsense and missense mutations that would be expected to destabilize the protein; blue, micro-deletions/insertions/duplications; orange, splice-site mutations; and black, regular missense mutations.

mutation. As shown in **Table 1**, very severe *SLC25A46*-related disease has been linked to mutations that yield markedly reduced SLC25A46 levels, including homozygous or compound heterozygous nonsense mutations, (c.691C>T, p.Arg231*; c.736A>T, p.Arg246*; c.42C>G, p.Tyr14*), a splice site variant (c.462+1G>A), and a micro-deletion (g.chr5: 110738771_11074670del). In addition, Wan et al. and Janer et al. verified that the three missense mutations c.1022T>C (p.Leu341Pro), c.998C>T (p.Pro333Leu), and c.425C>T (p. Thr142Ile) destabilize the protein without nonsense-mediated mRNA decay, causing a marked loss of SLC25A46 function. Such protein-depriving mutations lead to severe clinical symptoms of PCH or Leigh syndrome. In contrast, missense mutations of *SLC25A46* that are associated with normal or mildly reduced protein levels tend to result in a relatively mild phenotype. For instance, stable expression of the p.Gly249Asp mutant protein produces low-severity manifestations of optic atrophy spectrum disorder [17, 22] (**Table 1**). Thus, the more stable, functional, and abundant the mutant protein, the less severe the clinical manifestations.

In conclusion, the main molecular causes of *SLC25A46*-related neurological disease appear to be SLC25A46 loss of function or deficiency. The recessive inheritance pattern observed in all pathogenic *SLC25A46* mutation-affected individuals and families thus far contrast with the dominant inheritance pattern observed with other mitochondrial dynamic genes, including *OPA1*, *MFN1/2*, and *DRP1*, for which haplo-insufficiency and dominant negative effects are observed [8, 36, 37].

5. Pathophysiological function of SLC25A46

In the last 2 years, a series of experiments aiming at resolving the function of SLC25A46 and the pathogenesis of *SLC25A46*-associated diseases were conducted. Primary cultures of skin fibroblasts from HMSN6B patients (including PCH or Leigh syndrome patients) have been studied to investigate the pathophysiology of the diseases. Simultaneously, mutant SLC25A46 alleles or *SLC25A46*-targeted RNA-interference molecules were transfected into common cell lines (e.g., COS-7, HeLa, HEK293T, and HCT116) to study the consequences of the mutations or protein knock-down in a homogeneous genetic background. Finally, zebrafish, murine, and bovine models have been employed to examine the pathophysiological effects of *SLC25A46* mutations *in vivo* (**Table 2**).

5.1. Function of SLC25A46 in mitochondrial dynamics

In silico analysis led to the identification of a *SLC25A46* homolog in yeast, namely *Ugo1*. The Ugo1 protein is a modified mitochondrial solute carrier expressed in the mitochondrial outer membrane that operates as a mitochondrial fusion factor and interacts physically with Mgm1 (homolog of human OPA1) and Fzo (homolog of human MFN2) [38]. A succession of studies in cells demonstrated consistently that, like Ugo1, MTCH1, and MTCH2, SLC25A46 also localizes to the mitochondrial outer membrane [17, 20, 22].

Animal species	SLC25A46 mutations	SLC25A46 proteins	Age of onset	Age of death	Optic atrophy	Peripheral neuropathy	Ataxia	Degeneration in cerebellum /brainstem	Other features	Mitochondrial dynamics
Bovine Duchesne et al. [43]	c.376C>T	p. R126C	1 mo.	Euthanasia around 2–3 mo.	—	+	+	+	Degenerative lesions both in gray matter and white matter; demyelination in certain peripheral nerves.	Elongated mitochondria with abnormal cristae.
$Tg^{-/-}$ FVB/N mouse Duchesne et al. [43]	Tg18: indel 12 bp; Tg26: del 75 bp	p. Val122Leu123delinsATIIYI; p.Ala108fs*159	2 w	3–4 w	—	±	+	±	Impaired growth, small intestine, thymus, spleen and liver, severe hypoglycemia; low plasma iron concentrations combined with high ferritin.	Elongated mitochondria with abnormal cristae.
atc/atc C57BL/6 J mouse Terzenidou et al. [42]	c.283C>T	p.Gln95fs*	2 w	5 w	+	+	+	+	Growth retardation, severe thymic and splenic hypoplasia, compromised Purkinje cell dendritic arborization and reduced synaptic connectivity, RGC	Atypical mitochondria in Purkinje cells.

Animal species	SLC25A46 mutations	SLC25A46 proteins	Age of onset	Age of death	Optic atrophy	Peripheral neuropathy	Ataxia	Degeneration in cerebellum /brainstem	Other features	Mitochondrial dynamics
									aberrations, improper neuromuscular junction.	
$Slc^{-/-}$ B6D2 mouse Li et al. [39]	c.992_1037del	p.Leu331fs*346	2 w	2–8 w	+	+	+	+	Purkinje cell loss and dendritic abnormalities, degeneration in striatum, corpus callosum and spinal cord; axon degeneration and demyelination.	Enlarged or ring/C-shaped mitochondria.

Note: mo represents month; w the week.

Table 2. Clinical phenotypes associated with mutant SLC25A46 animal models.

Knock down of SLC25A46 in various cell lines by different research groups caused mitochondrial hyperfusion and abnormal cristae architecture visualized with fluorescent staining and electron microscopy [17, 20, 22]. In concordance, in an ultrastructural study of a SLC25A46 knock-out mouse model, we observed enlarged mitochondria with swollen cristae in Purkinje cell (PC) dendrites and sciatic nerves (**Table 2**) [39]. Hyperfused mitochondria consequent to SLC25A46 loss was unexpected because loss of Ugo1 function usually results in mitochondrial fission; however, it should be noted that strikingly similar cristae architecture abnormalities from loss of function are common to both genes [38, 40, 41]. Interestingly, in SLC25A46 mutant Purkinje cell bodies, ring-shaped or C-shaped mitochondria (a rarely reported morphology) were more commonly observed than hyperfused mitochondria [39, 42]. Furthermore, mitochondria were found to have an abnormal distribution and impaired movement within mutant Purkinje cells in a primary culture of mouse cerebellar cells [39]. These findings confirm that SLC25A46 plays an important role in the regulation of mitochondrial dynamics, including mitochondrial fusion/fission, distribution, and movement, as well as the maintenance of cristae architecture. Regarding the molecular actions of SLC25A46 in the balance of mitochondrial dynamics, recent research findings present three possible explanations: (1) SLC25A46 may act as an independent pro-fission factor; (2) SLC25A46 may serve as a regulator by interacting with mitochondrial fusion machinery, such as through an association with MFN1/2 oligomerization; and (3) SLC25A46 may regulate mitochondrial dynamics through its functions in lipid transfer between the endoplasmic reticulum (ER) and mitochondria.

In an inter-institution collaborative exploratory study employing immunoprecipitation assays and mass spectrometry analysis, there was no evidence of SLC25A46 interacting with MFN2 or OPA1 in HEK293T cells, but rather SLC25A46 was observed forming a complex with mitofilin that was independent of MFN2 [17]. Furthermore, overexpression of wild-type SLC25A46 protein led to mitochondrial fragmentation and disruption of the mitochondrial network. Thus, SLC25A46 was proposed to act as a pro-fission factor [17]. In contrast, two subsequent studies using similar immunoprecipitation approaches in patient fibroblasts and two cell lines (HEK293T with stable wild-type SLC25A46 expression and LAN5 neuronal cells) showed SLC25A46 interactions with proteins involved in fission and fusion, including MFN1/2 and OPA1, as well as with components of the MICOS (mitochondrial contact site and cristae organizing system) complex (**Figure 1**) [18, 20]. Moreover, decreased expression of SLC25A46 resulted in increased stability and oligomerization of MFN1 and MFN2 in association with mitochondria, thus promoting mitochondrial hyperfusion [18]. In SLC25A46 knock-out mice, two independent mass spectrometry studies yielded opposite results regarding the interaction between SLC25A46 and common dynamic proteins [42, 43]. Hence, although it seems reasonable that SLC25A46 would have interaction relationships with MFN1/MFN2 and the MICOS complex similar to those of Ugo1, further studies are needed to resolve its molecular mechanisms given the current conflicting results in the literature.

MFN2 tethers the ER to the mitochondrial network, suggesting that the ER may have a physical relationship with the mitochondrial network [44]. SLC25A46 has also been shown to interact with all nine components of the endoplasmic reticulum membrane complex (EMC) [18, 20], an ER protein complex recently shown to be necessary for phospholipid transfer from the ER to mitochondria in yeast. Most mitochondrial phospholipid species were altered

dramatically by the loss of SLC25A46, indicating that SLC25A46 provides direct coupling of lipid flux between the ER and mitochondria at outer-inner mitochondrial membrane contacts [20]. Meanwhile, endoplasmic reticulum chaperone BiP (a.k.a. 78 kDa glucose-regulated protein), which acts at the ER-mitochondria interface under stress conditions and is considered as a major regulator of the ER, was down-regulated in *SLC25A46* knock-out mice [43]. These findings support the notion that the facilitation of lipid flux at ER contact sites may be a primary function of SLC25A46.

Studies implicating OPA1 and the MICOS complex in the maintenance of cristae architecture are compelling, but it is unclear how they may interact [45]. The observation that SLC25A46 interacts with OPA1 and MIC60, the major MICOS organizer, provides a molecular link that may integrate their functions in modulating cristae architecture [18, 20].

It now seems likely that SLC25A46 may possess multiple homeostatic functions in mitochondrial dynamics. Further studies are expected to reveal more refined details of the pathophysiological functions of SLC25A46, such as which domain interacts with dynamic proteins and which domain recognizes and communicates with the ER.

5.2. Consequences of SLC25A46 dysfunction on mitochondrial metabolism

Disorganization of cristae leads to disruption of the assembly of the respiratory supercomplexes that mediate oxidative phosphorylation, which reduces the activity of their components (i.e., respiratory complexes I–V) and, thus, diminishes respiration efficiency [46, 47]. Mitochondrial metabolism is disrupted in both patients with mutant *SLC25A46* alleles and animal models of disrupted *SLC25A46*. Fibroblasts from patients harboring mutant *SLC25A46* showed varying extents of decreased oxygen consumption rate and glycolytic shift (decreased oxygen consumption rate-to-extracellular acidification rate ratio), consistent with the increased lactate levels indicated by magnetic resonance spectroscopy (MRS) [17]. Moreover, siRNA-mediated suppression of SLC25A46 in control fibroblasts phenocopied the basal oxygen consumption defect observed in the cells of patients with mutant *SLC25A46*, confirming a specific function of SLC25A46 in respiration [20]. Given the specificity of each tissue and each cell type in responding to physiological stresses and mutations, mitochondria isolated from the cerebellum of SLC25A46 knock-out mouse displayed a remarkable decrease in the activities of respiratory complexes I–IV, and thus a dramatically reduced ATP production potential [39]. Taken together, these observations support the hypothesis of an energetic defect being a principal cause of *SLC25A46*-related neurological disease.

5.3. SLC25A46 dysfunction in pathology

Mitochondrial pathobiology has long been linked to the pathogenesis of neurodegenerative diseases, in part because neurons are highly dependent upon mitochondrial metabolism. Autopsy on a pair of deceased siblings who died due to *SLC25A46* mutations showed a very small cerebellum, as well as degenerative changes in the inferior olive nucleus. Histology of the cervical spinal cord illustrated loss and ongoing degeneration of spinal motoneurons in the

medial anterior horn at all levels from the cervical to the lumbar region. Rectus femoris muscle biopsies showed severely atrophied muscle fibers of all types, without type grouping [48].

For now, most anatomical and histological analyses for *SLC25A46*-related diseases are based on animal models. Four *SLC25A46* mutant mammalian models have been discovered or designed, including a calf model and 3 mouse models with different genetic backgrounds (**Table 2**). Turning calf syndrome, a neurodegenerative disease, is characterized during massive inbreeding in cattle. Genetic study determines that this disease resulted from a single substitution in the coding region of the *SLC25A46* [43]. All affected calves manifested early onset of ataxia, especially of hind limbs, and paraparesis (2–6 weeks old). Despite symptomatic care, nervous symptoms progressed over the next months, leading to repetitive falls and ultimately resulting in permanent recumbency and inevitably euthanasia. Characteristic degenerative microscopic lesions were found in both gray matter (brainstem lateral vestibular nuclei and spinal cord thoracic nuclei) and white matter (dorsolateral and ventromedial funiculi of the spinal cord) regions of the central nervous system, as well as demyelination of some peripheral nerves [49]. Electron microscopy confirmed this neuropathy phenotype, revealing discrete demyelinating lesions and some enlarged nodes of Ranvier.

Three SLC25A46 knock-out mouse models with different genetic backgrounds, including FVB/N, C57BL/6J, and B6D2, were generated, respectively (**Table 2**). In spite of various mutation positions and sizes, three mouse lines displayed very similar phenotypes, including growth delay, progressive ataxia, optic atrophy, short life span, which recapitulated the pathological state in human. Further histopathologic studies have shown tissue- and cell-specific lesions in both the central nervous system and peripheral nervous system (**Table 2**).

Although macroscopic examination showed no overt abnormalities in the gross anatomy of mutant brain, histological staining revealed markedly reduced cerebellums, with Purkinje cells (PCs) that had stunted dendrites and were reduced in number. Degeneration (evidenced by Fluoro-Jade C dye) was selectively present in mutant PCs [39]. Examination via electron microscopy (EM) revealed that degenerated PC dendrites exhibited disorganized cytoskeleton, often containing remnants of mitochondria and other organelles. Numerous atypical mitochondria with cytoplasmic inclusions were found both in the soma and dendrites of PCs. In addition, a significant reduction in vGlut1 and vGlut2 immunoreactivity both in PCs and molecular layer indicated a paucity of glutamatergic synapses in mutant mice [42]. Apart from PCs, degenerative signals were also aggregated in the vestibular nucleus of brainstem, deep cerebellar nuclei, the striatum, the corpus callosum, and the spinal cord, but not in other parts of the brain [39]. The neurodegeneration was associated with astrogliosis and microgliosis in the cerebellum and spinal cord, indicating high levels of neuroinflammation [39, 42]. These observations suggest that although *SLC25A46* mRNA is transcribed in most neural tissues, SLC25A46 may have a tissue- or cell-specific function. Interestingly, mice with conditional knock-out *MFN2* or *DRP1* mutations showed a similar phenomenon, with major changes in cerebellar Purkinje cells, whereas granule cells seemed to be spared [50]. It is not yet known why specific neurons are selectively affected by mitochondrial dysfunction. It could be that a large neuronal size makes particular neurons susceptible; Purkinje cells are one of the largest neuron types in the brain with long axons and extremely extensive dendritic branches. Their

complex architecture requires the transport and distribution of highly organized organelles, including mitochondria.

Aged SLC25A46 mutant mice displayed enhanced hind limb clasping reflex and muscle atrophy, suggesting potential peripheral neuropathy. Acquiring compound muscle action potentials (CMAPs) reduced in mutant sciatic nerve measured by electromyography (EMG) *in vivo* [39]. Mutant peripheral nerves exhibited sporadic degenerative lesions with local macrophages containing lipid debris and signs of demyelination. In addition, the size of individual endplates in mutant mice was significantly reduced. Retarded neuromuscular junction maturation and improper innervation, early hallmarks of CMT2D, were also documented in mutant muscle [42]. All of these alterations are indicative of peripheral neuropathy.

Optical coherence tomography (OCT) scanning on retina for live mice revealed that although the optic discs were grossly normal in terms of retinal appearance, retinas were thinner in aged SLC25A46 mutant mice [39]. Further quantitative measurements indicated that ganglion cell complex (GCC) thicknesses, which includes the nerve fiber layer (NFL), ganglion cell layer (GCL), and inner plexiform layer (IPL), were significantly reduced in adult mutant mice. Retinal and these reductions were associated with retinal ganglion cell loss and atypically small optic nerve axons with reduced neurofilament expression, as well as some axons that exhibited signs of degeneration and demyelination [39, 42]. Pax6+ and GAD65+ GABAergic amacrine cells—both of which form synapses with retinal ganglion cells—were also significantly reduced. These pathological changes are in line with the phenotypic features of ADOA.

Ultrastructural studies revealed dysmorphic mitochondria in both the central and peripheral nervous systems. Numerous enlarged and round mitochondria with abnormal cristae were found in Purkinje cell dendrites, while ring- or C-shaped mitochondria were commonly observed in soma. Peripheral nerve axons also had abnormal round, fused, and aggregated mitochondria in myelinated and non-myelinated fibers [39, 43].

Given the degeneration in long peripheral axons and distal optic nerves of SLC25A46 knockout animal models, the aforementioned findings support the idea that neurons with long axons or complicated dendrites are more sensitive to abnormal mitochondrial dynamics. Similar to the findings in mutant Purkinje cells, this sensitivity could also be due to the impaired transport of hyperfused mitochondria along axons and dendrites, probably due to their abnormal size and/or reduced ATP availability in the distal portions of long axons secondary to mitochondrial dysfunction. Further studies are needed to clarify this point.

6. Conclusion

SLC25A46 plays a critical role in mitochondrial dynamics and the maintenance of mitochondrial cristae, which are particularly important in neurodevelopment and neurodegeneration. Loss of SLC25A46 function causes a wide spectrum of neurodegenerative diseases, including

optic atrophy, peripheral neuropathy, progressive ataxia, Leigh syndrome, and lethal congenital pontocerebellar hypoplasia. In SLC25A46-related neurodegenerative diseases, phenotype severity correlates strongly with the magnitude of SLC25A46 level deficit observed.

Acknowledgements

This work was supported by the Center for Pediatric Genomics at the Cincinnati Children's Hospital, a grant from the National Institutes of Health (1R01EY026609-01) to Taosheng Huang, and a grant from the National Natural Science Foundation of China (81470299) to Zhuo Li.

Conflict of interest

The authors declare that they have no conflicts of interest.

Author details

Zhuo Li[1,2], Jesse Slone[1], Lingqian Wu[2] and Taosheng Huang[1,3]*

*Address all correspondence to: taosheng.huang@cchmc.org

1 Division of Human Genetics, Cincinnati Children's Hospital Medical Center, Cincinnati, OH, USA

2 Center for Medical Genetics, School of Life Sciences, Central South University, Changsha, Hunan, China

3 Human Aging Research Institute, Nanchang University, Nanchang, Jiangxi, China

References

[1] Kann O, Kovacs R. Mitochondria and neuronal activity. American Journal of Physiology-Cell Physiology. 2007;**292**(2):C641-C657

[2] Chen H, Chan DC. Mitochondrial dynamics–fusion, fission, movement, and mitophagy–in neurodegenerative diseases. Human Molecular Genetics. 2009;**18**(R2):R169-R176

[3] Twig G, Hyde B, Shirihai OS. Mitochondrial fusion, fission and autophagy as a quality control axis: The bioenergetic view. Biochimica et Biophysica Acta. 2008;**1777**(9):1092-1097

[4] Su B, Wang X, Bonda D, Perry G, Smith M, Zhu X. Abnormal mitochondrial dynamics—A novel therapeutic target for Alzheimer's disease? Molecular Neurobiology. 2010;**41**(2-3): 87-96

[5] Zuchner S, Mersiyanova IV, Muglia M, Bissar-Tadmouri N, Rochelle J, Dadali EL, et al. Mutations in the mitochondrial GTPase mitofusin 2 cause Charcot-Marie-tooth neuropathy type 2A. Nature Genetics. 2004;**36**(5):449-451

[6] Lawson VH, Graham BV, Flanigan KM. Clinical and electrophysiologic features of CMT2A with mutations in the mitofusin 2 gene. Neurology. 2005;**65**(2):197-204

[7] Cartoni R, Martinou JC. Role of mitofusin 2 mutations in the physiopathology of Charcot-Marie-tooth disease type 2A. Experimental Neurology. 2009;**218**(2):268-273

[8] Olichon A, Guillou E, Delettre C, Landes T, Arnaune-Pelloquin L, Emorine LJ, et al. Mitochondrial dynamics and disease, OPA1. Biochimica et Biophysica Acta. 2006;**1763**(5-6): 500-509

[9] Alexander C, Votruba M, Pesch UE, Thiselton DL, Mayer S, Moore A, et al. OPA1, encoding a dynamin-related GTPase, is mutated in autosomal dominant optic atrophy linked to chromosome 3q28. Nature Genetics. 2000;**26**(2):211-215

[10] Delettre C, Lenaers G, Griffoin JM, Gigarel N, Lorenzo C, Belenguer P, et al. Nuclear gene OPA1, encoding a mitochondrial dynamin-related protein, is mutated in dominant optic atrophy. Nature Genetics. 2000;**26**(2):207-210

[11] Waterham HR, Koster J, van Roermund CW, Mooyer PA, Wanders RJ, Leonard JV. A lethal defect of mitochondrial and peroxisomal fission. New England Journal of Medicine. 2007;**356**(17):1736-1741

[12] Cassereau J, Codron P, Funalot B. Inherited peripheral neuropathies due to mitochondrial disorders. Revue Neurologique. 2014;**170**(5):366-374

[13] Sajic M. Mitochondrial dynamics in peripheral neuropathies. Antioxidants & Redox Signaling. 2014;**21**(4):601-620

[14] Schwarz TL. Mitochondrial trafficking in neurons. Cold Spring Harbor perspectives in biology. 2013;**5**(6):a011304

[15] Turnbull HE, Lax NZ, Diodato D, Ansorge O, Turnbull DM. The mitochondrial brain: From mitochondrial genome to neurodegeneration. Biochimica et Biophysica Acta. 2010; **1802**(1):111-121

[16] Archer SL. Mitochondrial dynamics—Mitochondrial fission and fusion in human diseases. New England Journal of Medicine. 2013;**369**(23):2236-2251

[17] Abrams AJ, Hufnagel RB, Rebelo A, Zanna C, Patel N, Gonzalez MA, et al. Mutations in SLC25A46, encoding a UGO1-like protein, cause an optic atrophy spectrum disorder. Nature Genetics. 2015;**47**(8):926-932

[18] Steffen J, Vashisht AA, Wan J, Jen JC, Claypool SM, Wohlschlegel JA, et al. Rapid degradation of mutant SLC25A46 by the ubiquitin-proteasome system results in MFN1/2-mediated hyperfusion of mitochondria. Molecular Biology of the Cell. 2017; **28**(5):600-612

[19] Charlesworth G, Balint B, Mencacci NE, Carr L, Wood NW, Bhatia KP. SLC25A46 mutations underlie progressive myoclonic ataxia with optic atrophy and neuropathy. Movement Disorders. 2016;**31**(8):1249-1251

[20] Janer A, Prudent J, Paupe V, Fahiminiya S, Majewski J, Sgarioto N, et al. SLC25A46 is required for mitochondrial lipid homeostasis and cristae maintenance and is responsible for Leigh syndrome. EMBO Molecular Medicine. 2016;**8**(9):1019-1038

[21] Nguyen M, Boesten I, Hellebrekers D, Mulder-den Hartog NM, de Coo I, Smeets H, et al. Novel pathogenic SLC25A46 splice-site mutation causes an optic atrophy spectrum disorder. Clinical Genetics. 2017;**91**(1):121-125

[22] Wan J, Steffen J, Yourshaw M, Mamsa H, Andersen E, Rudnik-Schoneborn S, et al. Loss of function of SLC25A46 causes lethal congenital pontocerebellar hypoplasia. Brain: A Journal of Neurology. 2016;**139**(11):2877-2890

[23] Hammer MB, Ding J, Mochel F, Eleuch-Fayache G, Charles P, Coutelier M, et al. SLC25A46 mutations associated with autosomal recessive cerebellar ataxia in north African families. Neuro-Degenerative Diseases. 2017;**17**(4-5):208-212

[24] Braunisch MC, Gallwitz H, Abicht A, Diebold I, Holinski-Feder E, Van Maldergem L, et al. Extension of the phenotype of biallelic loss-of-function mutations in SLC25A46 to the severe form of pontocerebellar hypoplasia type I. Clinical Genetics. 2018;**93**(2):255-265

[25] van Dijk T, Rudnik-Schoneborn S, Senderek J, Hajmousa G, Mei H, Dusl M, et al. Pontocerebellar hypoplasia with spinal muscular atrophy (PCH1): Identification of SLC25A46 mutations in the original Dutch PCH1 family. Brain. 2017;**140**(8):e46

[26] Sulaiman RA, Patel N, Alsharif H, Arold ST, Alkuraya FS. A novel mutation in SLC25A46 causes optic atrophy and progressive limb spasticity, with no cerebellar atrophy or axonal neuropathy. Clinical Genetics. 2017;**92**(2):230-231

[27] Haitina T, Lindblom J, Renstrom T, Fredriksson R. Fourteen novel human members of mitochondrial solute carrier family 25 (SLC25) widely expressed in the central nervous system. Genomics. 2006;**88**(6):779-790

[28] Palmieri F. The mitochondrial transporter family SLC25: Identification, properties and physiopathology. Molecular Aspects of Medicine. 2013;**34**(2-3):465-484

[29] Monne M, Palmieri F, Kunji ER. The substrate specificity of mitochondrial carriers: Mutagenesis revisited. Molecular Membrane Biology. 2013;**30**(2):149-159

[30] Palmieri F. Mitochondrial transporters of the SLC25 family and associated diseases: A review. Journal of Inherited Metabolic Disease. 2014;**37**(4):565-575

[31] Robinson AJ, Kunji ER. Mitochondrial carriers in the cytoplasmic state have a common substrate binding site. Proceedings of the National Academy of Sciences of the United States of America. 2006;**103**(8):2617-2622

[32] Kunji ER, Robinson AJ. The conserved substrate binding site of mitochondrial carriers. Biochimica et Biophysica Acta. 2006;**1757**(9-10):1237-1248

[33] Palmieri F, Monne M. Discoveries, metabolic roles and diseases of mitochondrial carriers: A review. Biochimica et Biophysica Acta. 2016;**1863**(10):2362-2378

[34] Yu-Wai-Man P, Griffiths PG, Hudson G, Chinnery PF. Inherited mitochondrial optic neuropathies. Journal of Medical Genetics. 2009;**46**(3):145-158

[35] Zuchner S, Vance JM. Emerging pathways for hereditary axonopathies. Journal of Molecular Medicine. 2005;**83**(12):935-943

[36] Feely SM, Laura M, Siskind CE, Sottile S, Davis M, Gibbons VS, et al. MFN2 mutations cause severe phenotypes in most patients with CMT2A. Neurology. 2011;**76**(20):1690-1696

[37] Fahrner JA, Liu R, Perry MS, Klein J, Chan DC. A novel de novo dominant negative mutation in DNM1L impairs mitochondrial fission and presents as childhood epileptic encephalopathy. American Journal of Medical Genetics Part A. 2016;**170**(8):2002-2011

[38] Sesaki H, Jensen RE. Ugo1p links the Fzo1p and Mgm1p GTPases for mitochondrial fusion. Journal of Biological Chemistry. 2004;**279**(27):28298-28303

[39] Li Z, Peng Y, Hufnagel RB, Hu YC, Zhao C, Queme LF, et al. Loss of SLC25A46 causes neurodegeneration by affecting mitochondrial dynamics and energy production in mice. Human Molecular Genetics. 2017;**26**(19):3776-3791

[40] Sesaki H, Jensen RE. UGO1 encodes an outer membrane protein required for mitochondrial fusion. Journal of Cell Biology. 2001;**152**(6):1123-1134

[41] Hoppins S, Horner J, Song C, McCaffery JM, Nunnari J. Mitochondrial outer and inner membrane fusion requires a modified carrier protein. Journal of Cell Biology. 2009;**184**(4): 569-581

[42] Terzenidou ME, Segklia A, Kano T, Papastefanaki F, Karakostas A, Charalambous M, et al. Novel insights into SLC25A46-related pathologies in a genetic mouse model. PLoS Genetics. 2017;**13**(4):e1006656

[43] Duchesne A, Vaiman A, Castille J, Beauvallet C, Gaignard P, Floriot S, et al. Bovine and murine models highlight novel roles for SLC25A46 in mitochondrial dynamics and metabolism, with implications for human and animal health. PLoS Genetics. 2017;**13**(4): e1006597

[44] Leal NS, Schreiner B, Pinho CM, Filadi R, Wiehager B, Karlstrom H, et al. Mitofusin-2 knockdown increases ER-mitochondria contact and decreases amyloid beta-peptide production. Journal of Cellular and Molecular Medicine. 2016;**20**(9):1686-1695

[45] van, der Laan M, Horvath SE, Pfanner N. Mitochondrial contact site and cristae organizing system. Current Opinion in Cell Biology. 2016;**41**:33-42

[46] Friedman JR, Mourier A, Yamada J, McCaffery JM, Nunnari J. MICOS coordinates with respiratory complexes and lipids to establish mitochondrial inner membrane architecture. eLife. 2015;**4**:e07739

[47] Cogliati S, Frezza C, Soriano ME, Varanita T, Quintana-Cabrera R, Corrado M, et al. Mitochondrial cristae shape determines respiratory chain supercomplexes assembly and respiratory efficiency. Cell. 2013;**155**(1):160-171

[48] Barth PG. Pontocerebellar hypoplasias. An overview of a group of inherited neurodegenerative disorders with fetal onset. Brain and Development. 1993;**15**(6):411-422

[49] Timsit E, Albaric O, Colle MA, Costiou P, Cesbron N, Bareille N, et al. Clinical and histopathologic characterization of a central and peripheral axonopathy in rouge-des-pres (Maine Anjou) calves. Journal of Veterinary Internal Medicine. 2011;**25**(2):386-392

[50] Chen H, McCaffery JM, Chan DC. Mitochondrial fusion protects against neurodegeneration in the cerebellum. Cell. 2007;**130**(3):548-562